Structural properties of InGaN/GaN/Al_2O_3 structure from reciprocal space mapping

A. Kursat Bilgili, Ömer Akpinar, Gürkan Kurtulus, M. Kemal Ozturk, Süleyman Ozcelik & Ekmel Ozbay

Journal of Materials Science: Materials in Electronics

ISSN 0957-4522
Volume 29
Number 14

J Mater Sci: Mater Electron (2018)
29:12373-12380
DOI 10.1007/s10854-018-9351-2

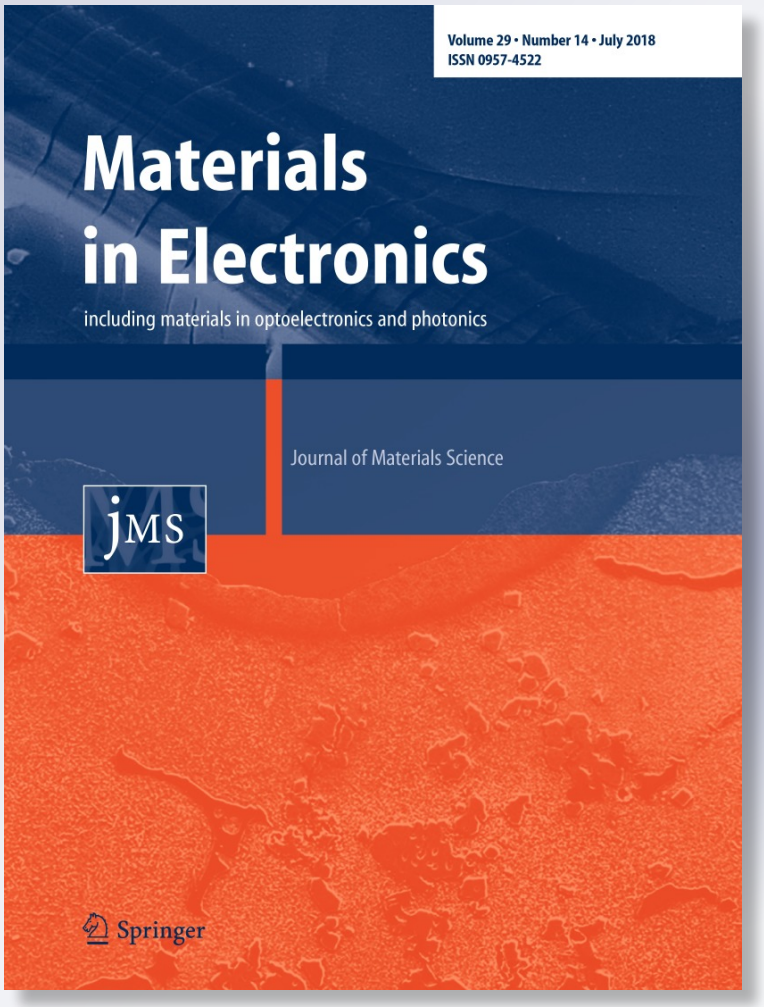

Springer

Your article is protected by copyright and all rights are held exclusively by Springer Science+Business Media, LLC, part of Springer Nature. This e-offprint is for personal use only and shall not be self-archived in electronic repositories. If you wish to self-archive your article, please use the accepted manuscript version for posting on your own website. You may further deposit the accepted manuscript version in any repository, provided it is only made publicly available 12 months after official publication or later and provided acknowledgement is given to the original source of publication and a link is inserted to the published article on Springer's website. The link must be accompanied by the following text: "The final publication is available at link.springer.com".

Author's personal copy

Journal of Materials Science: Materials in Electronics (2018) 29:12373–12380
https://doi.org/10.1007/s10854-018-9351-2

Structural properties of InGaN/GaN/Al_2O_3 structure from reciprocal space mapping

A. Kursat Bilgili[1] · Ömer Akpinar[1,2] · Gürkan Kurtulus[1,2] · M. Kemal Ozturk[1,2] · Süleyman Ozcelik[1,2] · Ekmel Ozbay[3]

Received: 12 March 2018 / Accepted: 23 May 2018 / Published online: 26 May 2018
© Springer Science+Business Media, LLC, part of Springer Nature 2018

Abstract
By using metal organic chemical vapor deposition technique, InGaN/GaN solar cell (SC) structure is deposited over sapphire (Al_2O_3) wafer as GaN buffer and GaN epitaxial layers. Structural properties of InGaN/GaN/Al_2O_3 SC structure is investigated by using high resolution X-ray diffraction technique dependent on In content. By using reciprocal space mapping, reciprocal space data are converted to w–θ data with a software. These w–θ data and full width at half maximum data are used for calculating lattice parameters. When compared with w–θ measurements in literature it is seen that especially a- lattice parameter is found very near to universal value from RSM. It is calculated as 3.2650 nm for sample A (S.A) GaN layer and 3.2570 nm for sample B (S.B) GaN layer on (105) asymmetric plane. Strain and stress calculations are made by using these lattice parameters. Strain and stress are calculated as 0.02363 and 8.6051 GPa for S.A GaN layer respectively. Other results are given in tables in the results and discussion section of this article. Edge, screw and mixed type dislocations are calculated as mosaic defects. All these calculations are made for two samples on (002) symmetric and (105) asymmetric planes. As a result it is seen that measurements by using RSM give more sensitive results. a- lattice parameter calculated with this technique is the best indicator of this result.

1 Introduction

Investigations show that there are nano-scale scientific studies today. Chemists and physicians have been trying with nano science for centuries. But as the result of recent studies the methods of science investigations are focused on applicable technology. Applications of nano science are called nano technology. Nano technology can be explained as, development of functional materials, devices, for controlling, understanding and production of physical, chemical and biological systems in nanometer scale. The uses of nano technology in industry are, micro censors, micro machines and constructing optoelectronic devices. Devices produced by using daily technology are, diodes, transistors, solar cells and microprocessors etc. In these devices semiconductors are used. Optoelectronic devices take place between ultraviolet and infrared region. III–V Nitrite semiconductors have a large application field today. Among III-nitrite semiconductors band gap range between (1.9–6.2 eV) forms a series for triple compounds [1, 2]. Metal organic chemical vapor deposition (MOCVD) system which do not need high vacuum takes attention in the growth of nitrite based structures such as InGaN and GaN. By the development of these materials, devices such as High electron mobility transistors (HEMT), laser diodes (LD), detectors, solar cells (SC) and light emitting diodes (LED) become more efficient. During the growth of these structures, every layer should be adjusted carefully and sensitively to form good performance devices.

In power electronics, because the power is delivered to an external circuit from an illuminated junction, it is found that it is possible to convert light energy to electrical energy. In fact, p–n junction SCs are used for supplying power for space satellites recently. SCs can supply power for these satellites for a long time and this is a great advantage according to batteries. SCs are formed in order to use present optical energy. During the formation of SCs convenient semiconductors are chosen for diffusion and ion deposition [3]. But applications of SCs

✉ A. Kursat Bilgili
sunkurt4@gmail.com

Ömer Akpinar
omerakpinar9@gmail.com

[1] Department of Physics, Gazi University, 06500 Ankara, Turkey

[2] Photonics Research Center, Gazi University, 06500 Ankara, Turkey

[3] Nanotechnology Research Center, Bilkent University, 06800 Ankara, Turkey

Author's personal copy

are not limited with space. Although intensity of solar light decrease because of atmosphere, by using SCs it is possible to use solar energy also on earth. During operation of a SC, high energy photons are absorbed, the electron–hole pairs (EHPs) formed are pushed towards the external circuit by the help of in-electrical field. During this process for example if we use a Si semiconductor the efficiency nearly 25%, but if a different material such as GaN is used, also by the effect of defects, efficiency decrease about 10% of this level. In this study electrical properties are not investigated. Instead of that structural defects which decrease the efficiency about 10% are examined for InGaN/GaN/Al_2O_3 SC structure.

InGaN/GaN structures are used as active layers in solar cell applications commonly [4, 5]. To form high quality solar cell structures and structural characterization of them is a very popular subject in recent studies. Because there are still some problems during growth of such structures, studies on these structures are going on continuously. Substrate temperature, layer growth duration and flux of the sources in MOCVD technique are effective growth conditions for forming high quality InGaN or GaN structures [6, 7].

Crystal quality, alloy compound, defects, strain, stress and many other structural properties can be determined by using XRD technique. For determining such parameters using High Resolution X-ray diffraction (HRXRD) technique is a good method to gain more sensitive results [8–10]. In this study, structural properties of InGaN/GaN solar cells are investigated by reciprocal space mapping (RSM) method. RSM is a sub-method of HRXRD. In classical HRXRD measurements there may be little shifts in peak positions causing from calibration mistakes. On the other hand, XRD patterns may be insufficient for the analysis of some structures which contain mixed and unseparated peaks. The biggest advantage of RSM is that even the mixed and unseparated peaks can be distinguished from each other. By the help of RSM more accurate results can be gained for structural parameters.

With good optimization of the device parameters during measurement and with fault percentages effecting rocking curves, peak angles, and interplanar spacing and lattice parameters can be determined with good accuracy. However, it is a better choice to prefer RSM to gain these parameters with perfect accuracy. In RSM, peaks on the plane can be seen clearly. In rocking curves, peak reflections in asymmetric planes may be evaluated as wrong by growing away from real peak values. Asymmetry here can be described as lose of intensity and disrupting of symmetry because of sample defects.

2 Experimental

In graded Sample A (S.A) and Sample B (S.B) InGaN/GaN nucleation layer SC structures are deposited on c- oriented sapphire (Al_2O_3) wafer by using MOCVD technique. Before growing the epitaxial film, in order to remove the dirts on the surface of the wafer, the film is cleaned for 10 min at 1100 °C temperature under H_2 atmosphere. After the cleaning process, epitaxial growth operation started by growing the GaN nucleation layer at 575 °C. During the growth operation flux ratio of TMGa (trimethylgallium) and NH_3 (ammonia) are adjusted as 10 and 1500 sccm respectively and the pressure is adjusted as 200 mbar. The thickness of this nucleation layer is 10 nm. After growth of the nucleation layer GaN buffer layer is grown over it at 1070 °C. Flux ratio of TMGa and NH_3 are adjusted as 15 and 1800 sccm during growth of this buffer layer and growth pressure is kept constant at 200 mbar. The thickness of this buffer layer is 1.6 µm. Growth operation continued by turning on the SiH_4 source and by the help of this source n type GaN layer is gained. In MOCVD technique SiH_4 source is dilute. The flux ratio of this SiH_4 source is 10 sccm. Graded and in graded $In_xGa_{1-x}N$ active layers are grown at 745–760 °C and in 75 sccm In flux ratio. The thickness of InGaN layers in S.A are 25 nm (graded) and 200 nm (graded). For S.B the thickness of InGaN layer is 220 nm (in graded). Active layers are grown between n type GaN with 1.9 µm and p type InGaN contact layers. P type InGaN layer is grown by using Mg doping source. The flux ratio of this source is 35 sccm. During the growth of InGaN layer other sources which were opened during growth of other layers are kept closed. In order to make more doping Mg flux ratio is adjusted as 40 sccm. In InGaN layers used as active layers In ratio is made graded by a continuous In flux ratio. Figure 1a shows the SC structure with graded InGaN layer and Fig. 1b shows the SC structure with in graded InGaN layer.

3 Results and discussion

XRD analysis of both samples is made with Bruker D8-Discover HRXRD device which has 1.540 Å wavelength $CuK_{\alpha 1}$ rays and Ge (220) oriented four crystal monocromator. In the measurement section of the device x, y, z, Φ and ξ axes are present together with θ and 2θ axes. These extra axes are used for maintaining the diffraction condition of symmetric and asymmetric planes. In this study, θ, 2θ, Φ and ξ axes are used for gaining reciprocal space map.

Reciprocal space mapping is a long procedure because of adjusting the axes which optimize the scanning.

In classical calculations, it is often seen in literature that using the results of rocking curves by detecting θ angle and

Author's personal copy

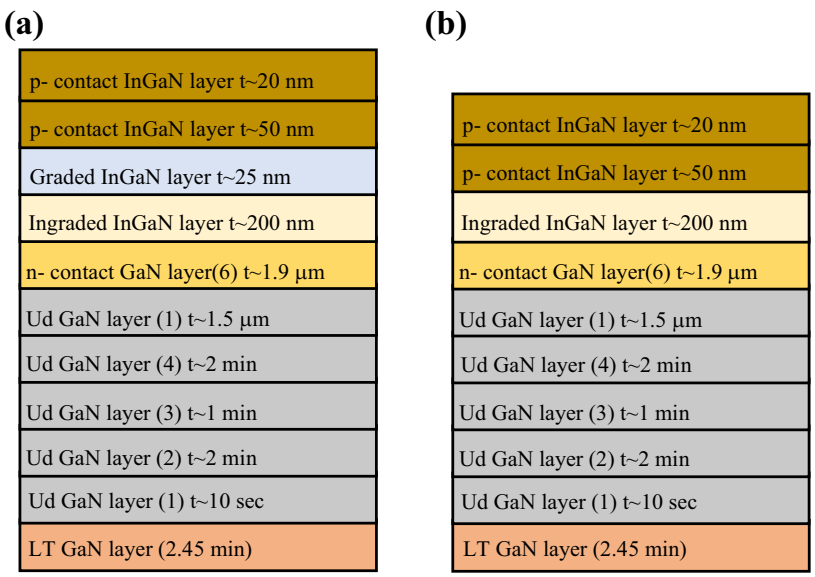

Fig. 1 **a** InGaN/GaN SC structure (S.A). **b** InGaN/GaN SC structure (S.B)

keeping 2θ diffraction angle constant in diffraction plane [11–13]. However, many factors are effective during the optimization of rocking curves. Optimizing bending of surface, adjusting the height of the sample and azimuthal adjusting are necessary for optimization. By good optimization of device as crystallographically, parameters needed can be measured with great accuracy. In classical methods, peak reflections in asymmetric planes, may cause faulty images by separation from real peaks. This situation can be summarized like the following; by perfect reflection of X-rays on planes symmetric interference peaks can be seen. Sometimes asymmetric peak loses its intensity and its symmetry deteriorate and these peaks forms a diffraction pattern. Classical XRD results are not as sensitive as RSM results for this reason classical XRD based comments on the analysis of the samples may cause inaccurate comments [14].

However, reciprocal space mapping is a good technique for calculating these parameters more sensitively and with high accuracy. Because reciprocal space maps are gained with slow scanning steps and more optimized adjusting. In reciprocal space maps it is possible to notice even the mixed plane peaks in great detail. These tricking diffraction patterns can be solved by reciprocal space mapping technique. By using reciprocal space mapping, investigation of mosaic defects with high accuracy is possible. Also, In ratio in InGaN layer in symmetric and asymmetric planes can be calculated accurately. Patterns gained from reciprocal space maps gives more detailed and certain images according to classical HRXRD peaks [14]. Mixed GaN and InGaN peaks can be recognized better with this technique.

In Fig. 2 reciprocal space maps of the samples are given for symmetric (002) and asymmetric (105) planes in two theta omega scanning mode. Here peaks of InGaN and GaN layers are scanned with wide offset values and later these offsets are eliminated according to the universal values of GaN. As can be seen symmetric peaks are more dominant in (002) plane.

If Fig. 2 is examined carefully, it can be seen that in reciprocal space maps it is easier to separate GaN and InGaN peaks from each other. As an example XRD pattern of S.A and S.B are given here for (002) symmetric plane. In Fig. 2a for (002) symmetric plane there is a slight InGaN peak on the left side of GaN peak, this situation is more obvious in reciprocal space map for (002) symmetric peak. In Fig. 2b it is almost impossible to notice InGaN peak. It seems as if there is no InGaN peak according to XRD pattern of (002) symmetric plane for S.B. However, if reciprocal space map of (002) symmetric peak for S.B is examined carefully it is possible to distinguish InGaN peak from GaN peak on the left of GaN peak. This is why reciprocal space mapping technique is a more convenient method for gaining more accurate results in structural calculations.

Nitrogenous compound and alloys such as GaN and InGaN have hexagonal crystal structures and their crystal quality can be measured by using broadening in symmetric peaks. Also, in such layers broadening of symmetric and asymmetric HR-XRD rocking scanning curves is caused from dislocations. Full width at half maximum (FWHM) values for GaN and InGaN layers are given in Table 1. It can be seen that peak position values are very near to each other. The reason for this may be similar growth conditions and In ratios in the alloys. When the values measured are compared for two samples, it is seen that asymmetric (105) values are nearly the same. This is because GaN layers for both samples have similar growth conditions. For (002) plane FWHM values for InGaN are compatible with those in literature. This result shows that InGaN layer in S.A has high crystal quality.

Author's personal copy

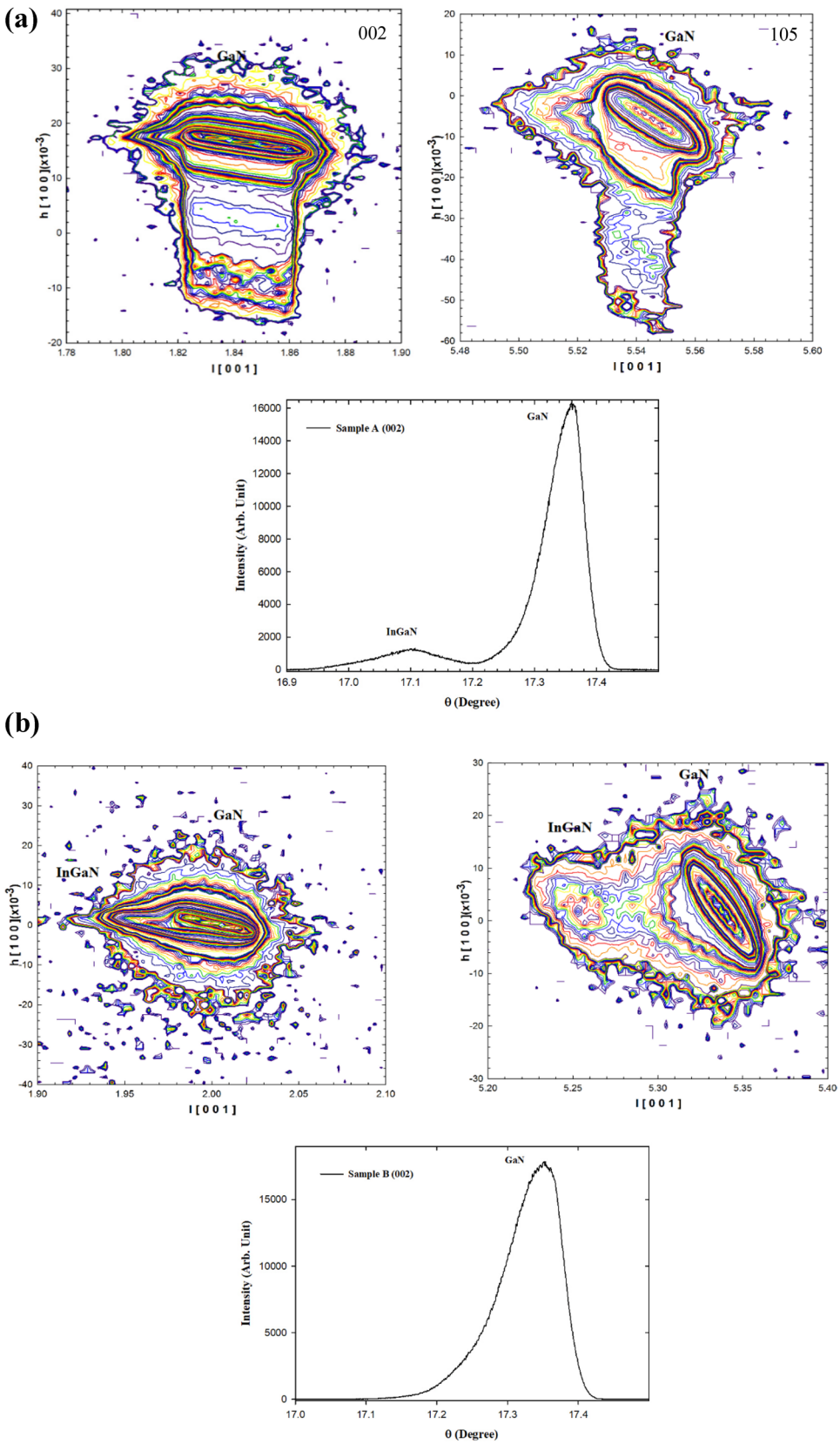

Fig. 2 Reciprocal space mapping XRD pattern of S.A and S.B for (002) and (105) planes. **a** RSM of S.A for (002), (105) planes and w–θ curve for S.A (002) plane respectively. **b** RSM of S.B for (002), (105) planes and w–θ curve for S.A (002) plane respectively

Author's personal copy

Table 1 Peak position values for GaN and InGaN layers in (002) and (105) planes for S.A and S.B

hkl	S.A	S.B
	Peak position (2θ)	Peak position (2θ)
(002) GaN	34.563	34.563
(002) InGaN	34.169	33.929
(105) GaN	105.006	105.006
(105) InGaN	104.241	104.319

Table 3 Lattice parameters for GaN and InGaN layers in (002) and (105) planes for S.A and S.B

Plane and compound	S.A		S.B	
	a (nm)	c (nm)	a (nm)	c (nm)
GaN (002)	–	0.51859	–	0.51859
InGaN (002)	–	0.52033	–	0.52033
GaN (105)	0.32650	0.51686	0.32570	0.51686
InGaN (105)	0.32650	0.51686	0.32650	0.51686

3.1 Lattice parameters

Calculation of lattice parameters has an important role in, strain, stress, edge and screw dislocation calculations. For hexagonal structures a- and c- lattice parameters should be calculated. The necessary formulas for calculating a- and c-lattice parameters are given in Eqs. (1) and (2).

$$c = \frac{\lambda l}{2 \sin\theta \cos\tau} \tag{1}$$

$$a = \frac{\lambda\sqrt{4/3}\sqrt{h^2 + hk + k^2}}{2 \sin\theta \sin\tau} \tag{2}$$

Here in Eqs. (1) and (2) lattice tilt angle τ can be calculated as $\tau = (\theta_+ - \theta_-)/2$ and θ Bragg angle can be calculated as $\theta = (\theta_+ + \theta_-)/2$. In Table 2 τ angle values corresponding to some symmetric and asymmetric planes are given.

Lattice parameters for InGaN layer can be calculated by using Vegard's law. The use of Vegard's law for InGaN layer lattice parameters is given in Eqs. (3) and (4).

$$a_{InGaN} = (x)a_{InN} + (1 - x)a_{GaN} \tag{3}$$

$$c_{InGaN} = (x)c_{InN} + (1 - x)c_{GaN} \tag{4}$$

Here x is the indium ratio in InGaN compound and it can be calculated with Eq. (5).

$$x = \frac{c_{0\ InGaN} - c_{0\ GaN}}{c_{0\ InN} - c_{0\ GaN}} \tag{5}$$

In contents for S.A are 10.5% and, 13.6% for S.B. Lattice parameters a- and c- for GaN and InGaN layers gained from Eqs. (1)–(4) are given in Table 3.

Table 2 τ angles corresponding to (101), (102), (106), (121) planes

(hkl)	τ (degree)
(101)	61.9599
(102)	43.1913
(106)	17.3763
(121)	78.6181

3.2 Strain and stress

Strain is described by reference lattice parameters c_0 and a_0. This is shown in Eqs. (6) and (7).

$$\varepsilon_c = \frac{c_{measured} - c_0}{c_0} \tag{6}$$

$$\varepsilon_a = \frac{a_{measured} - a_0}{a_0} \tag{7}$$

In bulk GaN hydrostatic strain is dominant. This is effected by doping and defects. Strain is usually caused by thin film-wafer thermal expansion coefficients or lattice mismatch. But when compared with typical strains the change in universal lattice parameters are high. Average reference values can be used but they are usually unreliable. It is possible for strain to have a negative value as in some parts of this work. Because it is randomized that how the dislocations will effect lattice parameters.

In-plane stress (σ) comes out during growth. This process includes doping, lattice mismatch and thermal expansion coefficient between film and wafer. Stress is usually calculated by measuring strain. If there is a strain situation that is rotationally symmetric, stress can be found by using strain. Stress formulas are given in Eqs. (8) and (9).

$$\varepsilon_a = \frac{\sigma^*(1 - \nu)}{E} \tag{8}$$

$$\varepsilon_c = \frac{\sigma^* \times 2 \times \nu}{E} \tag{9}$$

Here ν is the Poisson's ratio and it is taken as 0.212 and E is the Young modulus which is taken as 287 [15]. Values belonging to strain and stress are given in Table 4.

Strain and stress values are the same for S.A and S.B for (002) plane for that reason in Table 4, (b) only values for (105) is shown. In Table 3 it can be seen that lattice parameters are very similar to universal values. For this reason, strain and stress values gained from RSM method are also very near to universal values. This is true for both samples.

Determining the chemical composition in an alloy or compound is based on XRD technique. The relation between

Author's personal copy

Table 4 Strain and stress values for S.A and S.B

a_0 or c_0 (nm)	$a_{measured}$ or $c_{measured}$ (nm)	Strain	Stress (GPa)	Compound and plane
(a) Strain and stress values for S.A				
0.51855	0.51859	0.00008	0.0535	GaN (002) -c
0.52808	0.52033	−0.01467	−9.9275	InGaN (002) -c
0.51855	0.51686	−0.00325	−2.2021	GaN (105) -c
0.52807	0.51892	−0.01734	−11.7349	InGaN (105) -c
0.32262	0.32570	0.0096	3.4805	InGaN (105) -a
0.31896	0.32650	0.02363	8.6051	GaN (105) -a
(b) Strain and stress values for S.B				
0.51855	0.51860	0.00008	0.0535	GaN (105) -c
0.52807	0.51892	−0.01734	−11.7349	InGaN (105) -c
0.31896	0.32650	0.02363	8.6052	GaN (105) -a
0.32262	0.32570	0.00954	3.4771	InGaN (105) -a

lattice parameter and chemical compound is usually accepted to be linear. This linear relation is given by Vegard's law.

If nitrite alloy films belonging to functional group-III are grown on Al_2O_3 substrate directly, there may be problems and low quality crystal structure may occur. In order to prevent this situation a GaN buffer layer is grown onto the substrate [16, 17]. Approximately a perfect in-plane orientation comes out between GaN buffer layer and group-III nitrite layer. Here the buffer layer acts as a second substrate of relaxed GaN. If the thickness of the thin film is smaller than a critical value [18], they show a pseudomorphic action of growth and here basic planes of the hexagonal unit cells meet each other. In the basic plane of the heterostructure a strain comes out and it causes distortion in the hexagonal unit cell. As a result of this c/a ratio changes. This distortion may be explained by Hooke's law. z axis is parallel to c axis in the unit cell in epitaxial systems. This situation enables to simplify tensor for the elastical moduli [19, 20]. If there is biaxial strain, stress normal to the film surface disappears $\sigma_{33}=0$. By the help of this ε_{11}, the strain in the basic plane is obtained.

$$\varepsilon_{33} = -\frac{C_{13}}{C_{33}}(\varepsilon_{11} + \varepsilon_{22}) \tag{10}$$

Here σ_{ij} is stress, C_{ij} is elastical moduli in Voigt's notation and ε_{kl} is the strain. Strain is isotropic in basic plane, that is $\varepsilon_{11}=\varepsilon_{22}$. In relaxed films as well as pseudomorphic ones hexagonal structure is formed. According to the expressions for strain $\varepsilon_{33} = (c - c_0)/c_0$ and $\varepsilon_{11} = (a - a_0)/a_0$ according to these expressions (10) can be rewritten as;

$$\frac{c - c_0}{c_0} = -2\frac{c_{13}}{c_{33}}\frac{a - a_0}{a_0} \tag{11}$$

Here, c and a are lattice parameters belonging to strained InGaN film. $-c_0$ and $-a_0$ are relaxed lattice parameters. Strained lattice parameters are found from XRD data directly. Chemical composition is related with C_{13} and C_{33}. In hexagonal systems Poisson's ratio is calculated as;

$$\nu = 2\frac{C_{13}}{C_{33}} \tag{12}$$

A linear equation is solved for Poisson's ratio

$$\nu = x\nu(A) + (1 - x)\nu(B) \tag{13}$$

If a_0, c_0, and υ are inserted in (11), a cubic equation for x is gained

$$Px^3 + Qx^2 + Rx + S = 0 \tag{14}$$

Here:

$$P = (\nu(A) - \nu(B))(a_0(A) - a_0(B))(c_0(A) - c_0(B)) \tag{15}$$

$$Q = (1 + \nu(B))(a_0(A) - a_0(B))(c_0(A) - c_0(B)) + (\nu(A) - \nu(B))[a_0(A) - a_0(B))c_0(B) + (a_0(B) - a)(c_0(A) - c_0(B))] \tag{16}$$

$$R = (a_0(A) - a_0(B))[1 + \nu(B))c_0(B) - c] + (c_0(A) - c_0(B))[(1 + \nu(B))a_0(B) - \nu(B)a] + (\nu(A) - \nu(B))(a_0(B) - ac_0(B) \tag{17}$$

Author's personal copy

Table 5 Screw, edge type dislocation densities of the samples

Compound and plane	FWHM (deg.)	b_{edge}-c (nm)	b_{screw}-a (nm)	DB_{edge} (cm^{-2})	DB_{screw} (cm^{-2})
GaN (002) S.A	1.1690	0.5185	–	0.005648	–
InGaN (002) S.A	0.4359	0.5185	–	0.000785	–
GaN (105) S.A	0.2182	0.5185	0.3196	0.000197	0.000518
GaN (105) S.B	0.2173	0.5185	0.3196	0.000195	0.000514

$$S = (1 + \nu(B)a_0(B)c_0(B) - \nu(B)ac_0(B) - a_0(B)c \quad (18)$$

When the cubic equation is solved, by using the strained lattice parameters a and c, relaxed lattice parameters and In content x is determined. The coefficients in these equations for GaN and InN are $C_0^{GaN} = 0.51850$ nm, $a_0^{GaN} = 0.31892$ nm , $C_0^{InN} = 0.57033$ nm , $a_0^{InN} = 0.35387$ nm , GaN for $C_{13} = 103$ GPa , $C_{33} = 405$ GPa, for InN; $C_{13} = 92$ GPa, $C_{33} = 224$ GPa respectively [15]. The cubic equation has three real roots. But only one of them has physical meaning. x ratio value changes between one and zero. In content ratio x for InGaN layers are found as 9.82 and 15.11% for S.A and S.B respectively. When the accurate In ratio is calculated strain can also be calculated accurately. During the calculation of this accurate value RSM is very important. Peak shifts or offsets coming out during standard measurements can be prevented by RSM method. Strain values for InGaN layer in S.A are 2.68×10^{-3} c- and -3.37×10^{-3} on a-. The same values for S.B are 5.88×10^{-3} and -7.53×10^{-3} respectively. Strain calculations here are made according to reference value of InGaN and $\Delta x/x_0$ equation. Here $\Delta x = x - x_0$ and x, x_0 are strained and unstrained reference lattice parameters.

3.3 Dislocations

Edge, screw and mixed type dislocations can be calculated by a method found by Kurtz [17]. In this method dislocations are dependent on Burgers vector and FWHM value. Screw and edge type dislocations can be calculated with formulas (19) and (20).

$$D_B = \frac{\beta^2}{9\vec{b}_{edge}^{\,2}} \quad (19)$$

$$D_B = \frac{\beta^2}{9\vec{b}_{edge}^{\,2}} \quad (20)$$

Here β is the FWHM value and b is the length of Burgers vector. The length of the Burgers vector is taken as $\vec{b}_{screw} = 0.5185$ nm and $\vec{b}_{edge} = 0.3196$ nm [14]. The length of the Burgers vector is the same with lattice parameters. By using Burgers vector, edge type dislocations becomes suitable with azimuthal rotation of the crystals about normal of the surface. Mixed type dislocation is equal to the sum of screw type dislocations and edge type dislocations. This equation is shown in Eq. (21).

$$DB_{mixed} = DB_{screw} + DB_{edge} \quad (21)$$

The dislocation densities calculated are shown in Table 5. As Table 5 is investigated carefully edge and screw type dislocation density values are compatible with the ones in literature.

4 Conclusion

Structural properties of InGaN/GaN/Al_2O_3 solar cell device is investigated by using reciprocal space mapping technique. The reason for preferring RSM is that it gives more accurate results according to other type of scannings. This reality is also seen in this study. For example a- lattice parameters are found very near to reference values in literature. In literature the common value for a- lattice parameter is 0.31896 nm, in this study it is found as 0.32650 nm for both S.A and S.B. Mosaical defects are also determined. First RSM data is converted to w–θ data with LEPTOS software. Later with standard equations in XRD method, Strain, stress and dislocations are calculated. Strain is calculated by the help of lattice parameters gained from the RSM converted w–θ data. For example, strain value for GaN layer in (002) plane of S.A is found as 0.00008 and for InGaN layer in (105) plane of S.B it is found as 0.00954. In connection to this stress is calculated by the help of strain. Stress values for the layers and planes mentioned for strain are 0.0535 and 3.4771 GPa, respectively. Lattice parameters for InGaN layer is calculated with Vegard's law. In content is also calculated. And about dislocations; edge, screw and mixed type dislocation densities are calculated according to Kurtz's formula. For instance, for GaN layer in (002) plane, edge type dislocation is calculated as 0.005648 cm^{-2} for S.A. For the same layer in (105) asymmetric plane it is calculated as 0.000197 cm^{-2}. It is seen that all the values gained for stress, strain and dislocation densities are in accordance with previous works in literature done by different authors. As a result it is once more proved that RSM gives results with higher accuracy than any other method of structural studies in XRD technique.

Author's personal copy

References

1. S. Strite, H. Morkoc, Gan, Ain, and Inn: a review. J. Vac. Sci. Technol. B **10**(4), 1237–1266 (1992). https://doi.org/10.1116/1.585897
2. J.W. Orton, C.T. Foxon, Group III nitride semiconductors for short wavelength light-emitting devices. Rep. Prog. Phys. **61**(1), 1 (1998). https://doi.org/10.1088/0034-4885/61/1/001
3. B.G. Streetman, *Elements of Solid State Electronics, in Prentice Hall Solid State Physics Series* (Texas University, Austin, 1998), p. 0133356035
4. Y.D. Qi et al., Comparison of blue and green InGaN/GaN multiple-quantum-well light-emitting diodes grown by metalorganic vapor phase epitaxy. Appl. Phys. Lett. (2005). https://doi.org/10.1063/1.1866634
5. K.S. Ramaiah et al., A comparative study of blue, green and yellow light emitting diode structures grown by metal organic chemical vapor deposition. Solid-State Electron. **50**(2), 119–124 (2006). https://doi.org/10.1016/j.sse.2005.10.028
6. T.K. Kim et al., Influence of growth parameters on the properties of InGaN/GaN multiple quantum well grown by metalorganic chemical vapor deposition. Curr. Appl. Phys. **7**(5), 469–473 (2007). https://doi.org/10.1063/1.4841575
7. Y. Nanishi, Y. Saito, T. Yamaguchi, RF-molecular beam epitaxy growth and properties of InN and related alloys. Japn. J. Appl. Phys. 1 **42**(5a), 2549–2559 (2003)
8. J. Singh, *Electronic and Optoelectronic Properties of semiconductor Structures* (Cambridge University Press, New York, 2003)
9. G. Bauer, W. Richter, *Optical Characterization of Epitaxial Semiconductor Layers* (Springer, Berlin, 1996). ISBN 978-3-642-79678-4
10. D.K. Bower, B.K. Tanner, *High Resolution X-ray Diffractometry and Topography* (Taylor & Francis Group, London, 2002). ISBN 9780850667585
11. M.K. Ozturk et al., Structural analysis of an InGaN/GaN based light emitting diode by X-ray diffraction. J. Mater. Sci. Mater. Electron. **21**(2), 185–191 (2010)
12. M.K. Ozturk et al., Strain-stress analysis of AlGaN/GaN heterostructures with and without an AlN buffer and interlayer. Strain **47**, 19–27 (2011). https://doi.org/10.1111/j.1475-1305.2009.00730.x
13. C. Kisielowski, Strain in GaN thin films and heterostructures. Semiconductors Semimetals **57**, 275–317 (1999)
14. Y. Bas, *$In_xGa_{1-x}N$ (x = 0.075; 0.090; 0.100) Mavi LED'lerin Mikroyapısal Kusurlarının Ters Örgü Uzay Haritası İle İncelenmesi* (Gazi University, Ankara, 2015)
15. M.A. Moram, M.E. Vickers, X-ray diffraction of III-nitrides. Rep. Prog. Phys. **72**(3), 036502 (2009)
16. M. Schuster et al., Determination of the chemical composition of distorted InGaN GaN heterostructures from X-ray diffraction data. J. Phys. D **32**(10a), A56–A60 (1999)
17. B.G. Streetmann, *Solid State Electronics Devices* (Prentice-Hall, Inc., Upper Saddle River, 1995)
18. S. Nakamura, Gan growth using gan buffer layer. Japn. J. Appl. Phys. 2 **30**(10a), L1705–L1707 (1991)
19. S.M. Sze, *Semiconductor Devices, Physics and Technology* (Wiley, New York, 2002)
20. R. Chierchia et al., Microstructure of heteroepitaxial GaN revealed by X-ray diffraction. J. Appl. Phys. **93**(11), 8918–8925 (2003)